

# On the suitability of redundant accelerometers for the implementation of smart oscillation monitoring system: Preliminary assessment

Giorgio de Alteriis<sup>1</sup>, Enzo Caputo<sup>1</sup>, Rosario Schiano Lo Moriello<sup>1</sup>

<sup>1</sup> Department of Industrial Engineering, University of Naples Federico II, Piazzale Tecchio 80, 80125, Naples, Italy

## ABSTRACT

Structural health monitoring (SHM) is an essential aspect to ensure the safety and longevity of civil infrastructure. In recent years, there has been a growing interest in developing SHM systems based on Micro-Electro-Mechanical Systems (MEMS) technology. MEMS-based sensors are small, low-power, and cost-effective, making them ideal for large-scale deployment in structural monitoring systems. However, the use of MEMS-based sensors in SHM systems can be challenging due to their inherent errors, such as drift, noise, and bias instability; these errors can affect the accuracy and reliability of the measured data, leading to false alarms or missed detections. Therefore, several methods have been proposed to compensate for these errors and improve the performance of MEMS-based SHM systems. For this purpose, the authors propose the combined of a redundant configuration of cost-effective MEMS accelerometers and a Kalman Filter approach to compensate MEMS inertial sensor errors and data filtering; the performance of the method is preliminarily assessed by means of a custom-controlled oscillation generator and compared with that granted by a high-cost, high-performance MEMS reference system where amplitude differences of 0.02 m/s<sup>2</sup> have been experienced. Finally, a sensor node for real-time monitoring has been proposed that exploits LoRaWAN and NFC protocols to access the structure information to be monitored.

**Section:** RESEARCH PAPER

**Keywords:** structural monitoring systems; oscillation measurements; Kalman filter; zero-velocity update; accelerometers; Internet of Things

**Citation:** Giorgio de Alteriis, Enzo Caputo, Rosario Schiano Lo Moriello, On the suitability of redundant accelerometers for the implementation of smart oscillation monitoring system: Preliminary assessment, Acta IMEKO, vol. 12, no. 2, article 11, June 2023, identifier: IMEKO-ACTA-12 (2023)-02-11

**Section Editor:** Laura Fabbiano, Politecnico di Bari, Italy

**Received** April 4, 2023; **In final form** April 18, 2023; **Published** June 2023

**Copyright:** This is an open-access article distributed under the terms of the Creative Commons Attribution 3.0 License, which permits unrestricted use, distribution, and reproduction in any medium, provided the original author and source are credited.

**Funding:** This work was supported by PON "RESEARCH AND INNOVATION" 2014-2020 and FSC ", project: "Intelligent Monitoring System for the Safety of Urban Infrastructures (INSIST)", CUP: E64E18000110005.

**Corresponding author:** Giorgio de Alteriis, e-mail: [giorgio.dealteriis@unina.it](mailto:giorgio.dealteriis@unina.it)

## 1. INTRODUCTION

The detection of the stress state of structures is an important problem in the field of structural engineering as it provides crucial information for monitoring their health and detecting the development and propagation of damage within them. Structural Health Monitoring (SHM), which encompasses a variety of techniques and technologies, has been developed to address this issue and is widely used in both aerospace and civil engineering [1]–[7].

In recent decades, SHM has extended its applications to infrastructure and civil engineering, including historic and new buildings, bridges, tunnels, industrial plants, manufacturing facilities, offshore platforms, port structures, foundations, and excavations [8]–[11].

Existing bridge structures are exposed to various environmental and operational stresses during their lifetime, and the influences of these external loads can lead to the acceleration of structural damage. In addition, extreme events such as earthquakes can occur during the life of a bridge, emphasizing the need for timely detection of the structure's condition to ensure safety. While visual inspection has traditionally played an important role in detecting defects on the structure surface and assessing the structural condition, it is labor-intensive, time-consuming, and subjective. To address this issue, SHM techniques have been proposed and are increasingly applied to long-span bridges [12]–[14]. SHM is defined as the use of sensing techniques and analysis of structural features to detect structural damage or deterioration; it is suggested that SHM should be considered in the context of condition assessment and as a damage detection technique [15]. In summary, the main

objectives of SHM are damage detection and condition assessment.

SHM techniques have been applied to bridges for almost 40 years through the installation of Structural Health Monitoring Systems (SHMS) and have been increasingly applied to long-span bridges worldwide. In summary, SHM techniques, particularly those based on vibration measurements, have great potential in the monitoring and maintenance of bridges to ensure their safety and longevity [16]–[20]. Among the various sensor techniques used in SHM, vibration-based measurement using accelerometers and data acquisition systems is one of the most widely studied and applied methods. In this approach, the response of the structure is measured under a given excitation, and its modal parameters, such as natural frequencies, damping ratios, mode shapes, and modal scaling factors, are determined [21]–[23]. The performance of the accelerometer is critical to the quality of the acquired data and the accuracy of the results. Therefore, the proper selection of the accelerometer should consider the balance between the cost and performance of the overall SHM system [24], [25].

In recent years, the use of micro-electromechanical systems (MEMS) sensors in SHM systems has gained significant attention. MEMS sensors are tiny devices that can measure a wide range of physical quantities, such as acceleration, strain, pressure, and temperature, with high accuracy and precision [26]. They are also compact, low-power, and cost-effective, making them ideal for large-scale and long-term monitoring of structures. The integration of MEMS sensors into SHM systems brings several benefits, such as improved accuracy and reliability, reduced power consumption, and enhanced data acquisition and processing capabilities. MEMS sensors can provide real-time data on the stress state of a structure, enabling early detection of damage or deterioration and allowing for timely and cost-effective maintenance and repair. They can also be used to identify potential failure modes and predict the remaining useful life of the structure. In the case of bridges, the use of MEMS sensors in SHM systems can provide a comprehensive and continuous monitoring solution that can detect even subtle changes in the structure's condition due to external loads, traffic, or environmental factors [24], [27]. This information can be used to optimize the bridge's performance and extend its service life while reducing maintenance and repair costs and ensuring the safety of the users.

Overall, the use of MEMS sensors in SHM systems represents a promising approach for the monitoring and maintenance of structures, particularly in the case of large-scale and critical infrastructure such as bridges [28]. With further advances in MEMS technology and data analytics, it is expected that SHM systems will become even more efficient, accurate, and cost-effective, providing greater benefits to both engineers and end-users.

MEMS inertial sensors offer several advantages, but it is important to consider their drawbacks as well. Their small size makes them highly sensitive to environmental changes, and random noise can make error compensation procedures more complex and limit their applicability [29], [30]. An increasing bias drift with non-linear characteristics is a significant factor to consider, as it demonstrates that while MEMS IMUs can provide remarkable accuracy at high rates, angular velocity, and acceleration data can easily degrade over longer periods. Therefore, special attention must be paid to these sensors, which are typically classified based on their bias instability and random walk parameters, both of which characterize their performance

and suitability for specific applications [31], [32]. For example, accelerometers with a bias instability lower than 0.01 mg are considered "marine-grade," while more cost-effective "consumer-grade" sensors have lower performance but also lower power consumption [33]–[35].

To overcome the MEMS limitations, several studies have been conducted on the adoption of a Kalman filter (KF) to compensate the MEMS errors. In particular, for SHM applications, high-frequency noise could be a key element to accurately estimate the structure acceleration. So, the Kalman Filter algorithm can be used to reduce noise in data obtained from MEMS accelerometers. It works by estimating the state of a system based on a series of noisy measurements. In the case of MEMS accelerometer data, the Kalman filter can be used to estimate the true acceleration of an object by filtering out high-frequency noise [36]–[39].

In this research, a redundant prototype of low-cost accelerometers that exploits a Kalman Filter algorithm for filtering purposes has been proposed. Then, the performance of the proposed solution is assessed by means of a comparison with a high-performance accelerometer sensor by means of a controlled oscillation generator that is specifically realized to obtain oscillations with known frequency and amplitude. Finally, the authors propose a sensor node that could be adopted for SHM applications.

The paper is organized as follows; the proposed method, the implementation of the controlled oscillation generator, and the sensor node realized are described in Section 2, while in Section 3, the system architecture that includes both the hardware and software implementation has been described. Finally, in Section 4 the obtained results are presented as advantages introduced by the proposed approach, the overall performance reached in oscillation measurements, and the proposed IoT architecture before drawing the conclusions in Section 5.

## 2. PROPOSED METHODS AND SMART MONITORING ARCHITECTURE

A platform based on the Internet of Things (IoT) exploiting redundant low-cost MEMS accelerometers for monitoring large structures such as bridges and tunnels has been evaluated, where the redundant prototype is already presented in [40]. The research activities have been focused mainly on two main aspects: (i) a prototype of redundant low-cost MEMS accelerometers evaluation for oscillation measurements by exploiting the Kalman filter for data filtering, where the performance is assessed by means of custom testing setup for controlled oscillation measurements and a result comparisons with a reference system, i.e., high-performance accelerometer sensor; (ii) an IoT solution for a real-time system that acquires and visualizes data based on the adoption of the redundant prototype and the typical protocol of IoT.

### 2.1. Proposed method

Regarding the first point, the main goal was to use a redundant configuration of accelerometers to reduce the typical errors that affect low-cost MEMS accelerometer sensors, such as bias instability, in-run bias instability, and velocity random walk. In this way, thanks to the redundant prototype performances, it could be adopted for oscillation measurements. To this aim, the authors propose an initialization procedure based on the adoption of a Zero-Velocity Update (ZVU) filter that allows to estimate of the initial error values and the initial alignment. In

this way, the acceleration measurements are compensated by the estimated noise values and then are processed by means of a Kalman Filter for high-frequency noise reduction and, finally, a Fast Fourier Transform (FFT) to evaluate the oscillation frequency and amplitude, as shown in Figure 1. The performance validation of the proposed method is assessed by a suitably controlled oscillation generator based on a crank-rod system capable to emulate different oscillation frequencies. Finally, a marine-grade MEMS sensor has been adopted as a reference system to assess and compare the performance reached by the proposed solution.

### 2.1.1. Zero-Velocity Update filter and initial alignment

The Kalman filter is a recursive algorithm that can be used to estimate the state of a dynamic system based on a series of noisy measurements. It works by predicting the state of the system at the next time step based on a model of the system dynamics and then updating this prediction based on the actual measurements. The algorithm includes two key steps: prediction and update. In the prediction step, the state estimate and error covariance matrix is predicted based on the previous state estimate, control input, and system dynamics. In the update step, these predictions are updated based on the actual measurements and the measurement noise covariance matrix [32].

The ZVU filter is based on an Error-State Kalman Filter (ESKF). This approach is based on the assumption that the system output is in a standing condition, i.e., the velocity is equal to zero. The ZVU filter is realized according to the following steps:

- 1) the position vector is provided by a GNSS source;
- 2) the velocity vector is set equal to zero;
- 3) roll and pitch angles are obtained by means of a coarse leveling procedure according to (1) and (2):

$$\theta = \arctan\left(\frac{-f_{ib,x}^b}{\sqrt{(f_{ib,y}^b)^2 + (f_{ib,z}^b)^2}}\right) \quad (1)$$

$$\phi = \arctan2(-f_{ib,y}^b, -f_{ib,z}^b), \quad (2)$$

where  $\theta$  is the pitch angle,  $\phi$  is the roll angle,  $f_{ib}^b$  represents the raw acceleration measurements among the x, y, and z axis referred to as the body reference frame.

The predict/correct phases are realized according to the ESKF implementation [40]; in this way, noise terms are estimated during the state vector correction and exploited in the successive prediction stages. The residual error values are then adopted to correct the acceleration measurements to obtain better performance in frequency and amplitude oscillation measurements.

For the sake of clarity, in this specific application, the GNSS position is only once evaluated; in fact, the accelerometer sensors are mounted on a structure where the GNSS position variations are not significant or not observable by most GNSS modules. Regardless, knowledge of the position is necessary to accurately compensate for the gravity vector.

### 2.1.2. Kalman Filter approach

Once obtained, the initial noise parameters, thanks to the application of the ZVU, and a further KF has been applied to the acquired acceleration samples in order to filter out high-frequency noise. To suitably reduce the computational burden, the update matrix is reduced to the identity matrix (i.e., in the prediction stage, the so-called a-priori estimated value  $\hat{x}^-$  is equal to the corrected value obtained in the previous iteration). As for the correction stage, it is obtained according to the following equations:

$$K = P/(P + R) \quad (3)$$

$$\hat{x}^+ = \hat{x}^- + K(x - \hat{x}^-) \quad (4)$$

$$P = (I - K)P + (\hat{x}^+ - \hat{x}^-)Q, \quad (5)$$

where  $K$  is the Kalman gain,  $P$  is the error covariance matrix,  $R$  is the noise covariance matrix,  $\hat{x}$  and  $\hat{x}^-$  are the state vector and estimated state vector, respectively, i.e., the acceleration measurements,  $I$  is the identity matrix, and  $Q$  is the system noise covariance matrix.

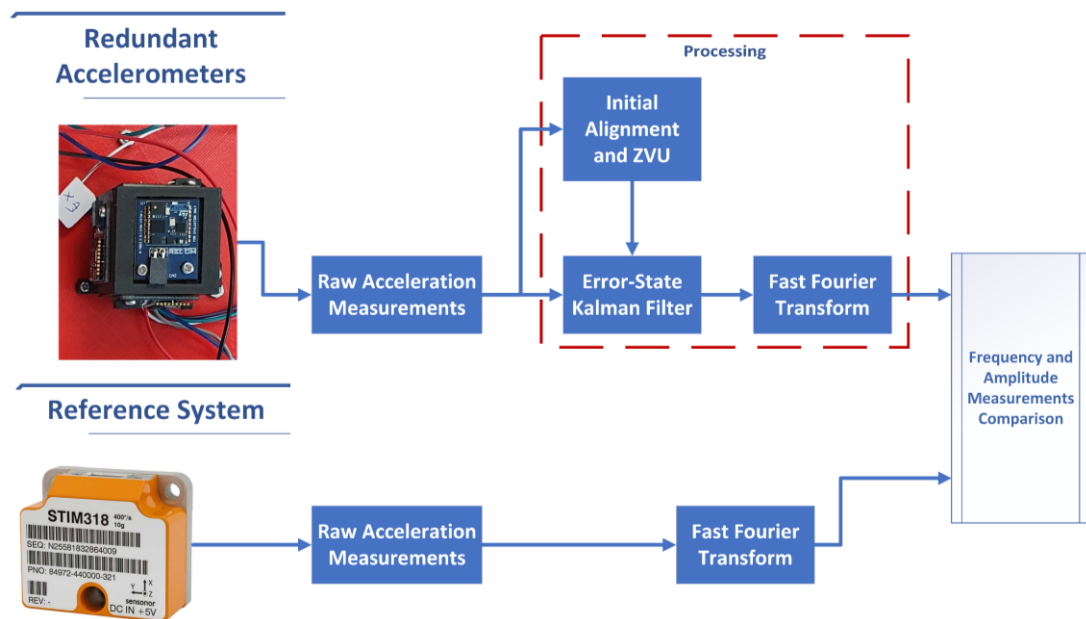


Figure 1. Proposed method based on the adoption of a Zero Velocity Update filter.

### 2.1.3. Controlled oscillation system and measurement setup

The measurement setup is composed of a controlled stepper motor that rotates a cylinder that is connected to the beam by means of a linkage in such a way as to convert the rotary motion of the stepper motor into linear motion. The sensor modules are placed on a plate rigidly constrained to the beam; in this way, harmonic motion is realized. The nominal acceleration values ( $a(t)$ ) can be derived from the maximum imposed displacement and frequency by the equation:

$$a(t) = -\omega^2 A \sin(\omega t), \quad (6)$$

where  $A$  is the vertical displacement amplitude,  $\omega = 2\pi f$  is the angular frequency.

The geometrical dimensions of the realized system are reported in Table 1, where it is also highlighted the maximum displacement that is evaluated as the difference between the highest and lower points of the plate (among the Z-Axis).

Figure 2 shows the controlled oscillation generator and the measurement setup. In particular, the mechanical parts are realized by the 3D printing process [41], [42] and are highlighted in black color, while the stepper motor and motor driver are highlighted in orange color. The measurement setup is mainly composed of the sensor modules, i.e., the proposed redundant low-cost accelerometers (red) as well as the STIM318 by SensoNor™, the marine-grade (green) accelerometer exploited as a comparison reference. Both modules are connected to a microcontroller (placed under the plate), specifically, the STM32F446RE from STMicroelectronics™, that acquires data via the I2C (Inter Integrated Circuit) and via the UART protocol, respectively. To this aim, an interface between the RS422 and UART protocols was realized using dual differential drivers and receivers (SN75C1167 from Texas Instruments). To synchronize the two systems, the microcontroller provides an external trigger to sample the marine-grade accelerometer data. The STIM318 acquires data at 2 kHz and is triggered at 125 Hz, resulting in a mean delay of 250 μs between the request and sampling of measured quantities. Finally, the acquired data is sent to a personal computer for further processing via a Bluetooth module connected to the microcontroller through the UART interface.

Table 1. Geometrical dimension of the controlled oscillating system.

System	Dimension (cm)
Beam	22.5 × 1 × 1 (L × W × H)
Linkage	9.5 × 0.2 × 0.5 (L × W × H)
Cylinder radius	5.5
Max Displacement	0.5

### 2.2. Proposed smart monitoring architecture

As for the second point, the prototype device is completed with a wireless communication system based on the LoRaWAN protocol and a NFC module for remote and in-situ monitoring, respectively, as shown in Figure 3. Once the operations for determining the quantities of interest have been locally performed, the microcontroller sends the result via LoRaWAN protocol to a gateway on which a node-red-flow is implemented that forwards the measured data via MQTT to a Thingsboard-based cloud dashboard. Moreover, the data are also accessible through NFC protocol. In particular, using a mobile phone as NFC reader, the identity of the node is detected and exploited to access the IoT platform and display measured data on the mobile application.

The proposed architecture aims to transmit only the maximum amplitude value of the signal, which is evaluated by the microcontroller as the peak in the frequency domain. The microcontroller then sends both the frequency and amplitude values, effectively reducing the number of samples transmitted and allowing for real-time monitoring. This ensures that only relevant information is transmitted, resulting in a more efficient system protocol with fewer packets, for forwarding measured data via the LoRa and NFC protocol so as to speed up NFC and Dashboard communications.

### 3. SYSTEM ARCHITECTURE

The hardware components used in performance assessment and wireless sensor node development for real-time monitoring are reported in Table 2 and Table 3, respectively, while the corresponding operations flow-chart are shown in Figure 4a and Figure 4b. For the sake of clarity, the redundant prototype is composed of six iNemos from STMicroelectronics™ in a cubic configuration.

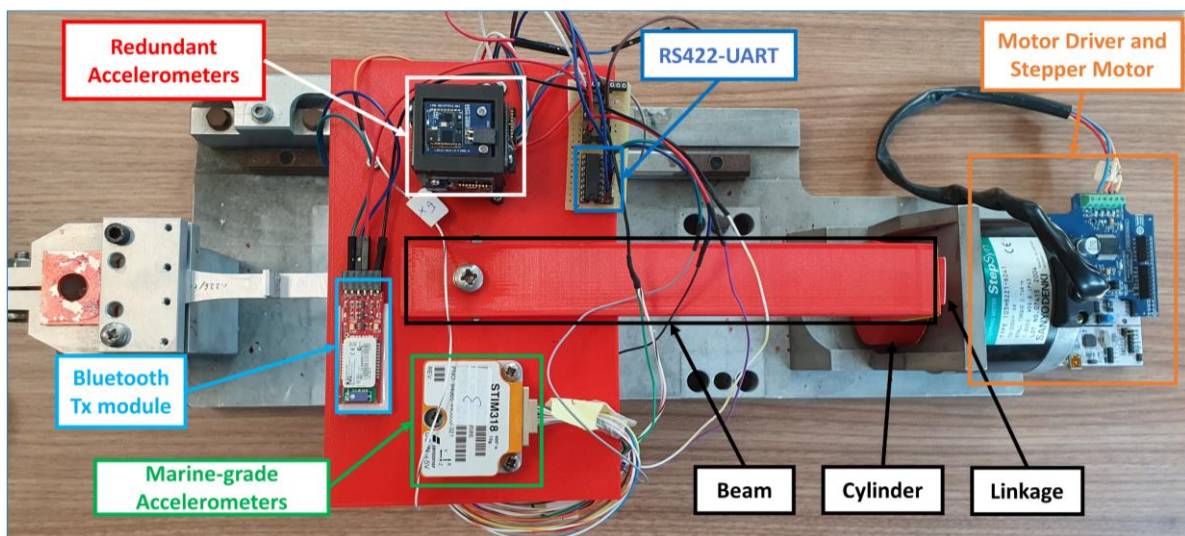


Figure 2. Realized oscillating system and measurement setup for performance assessment; thanks to the stepper motor oscillations with known frequency and amplitude can be applied to the low-cost redundant accelerometers.

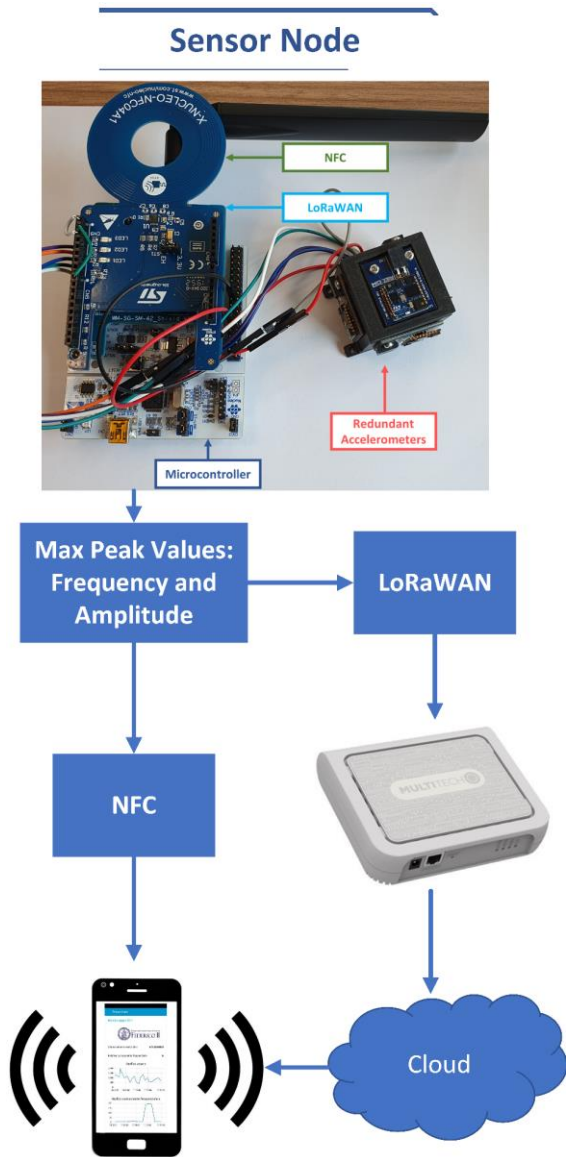


Figure 3. Sensor node and proposed smart monitoring architecture.

Table 2. Performance evaluation equipment.

Hardware	Part number	Manufacturer
Redundant Accelerometers	LSM6DSM (Six iNemos)	STMicroelectronics
Marine-grade accelerometers	STIM318	SensoNor
Microcontroller	Nucleo-F446RE	STMicroelectronics
Motor	StepSyn	SANYO DENKI
Motor Driver board	X-NUCLEO-IHM04A1	STMicroelectronics
Bluetooth module	RN41	Roving
RS422-UART	SN75C1167	Texas Instruments

Table 3. Sensor node realization hardware.

Hardware	Part number	Manufacturer
Microcontroller	Nucleo-F446RE	STMicroelectronics
Sensor board	X-Nucleo-IKS02A1	
NFC module	X-NUCLEO-NFC04A1	
LoRA module	I-NUCLEO-LRWAN	
SPI-micro Sd-Card	410-380	Diligent Inc.

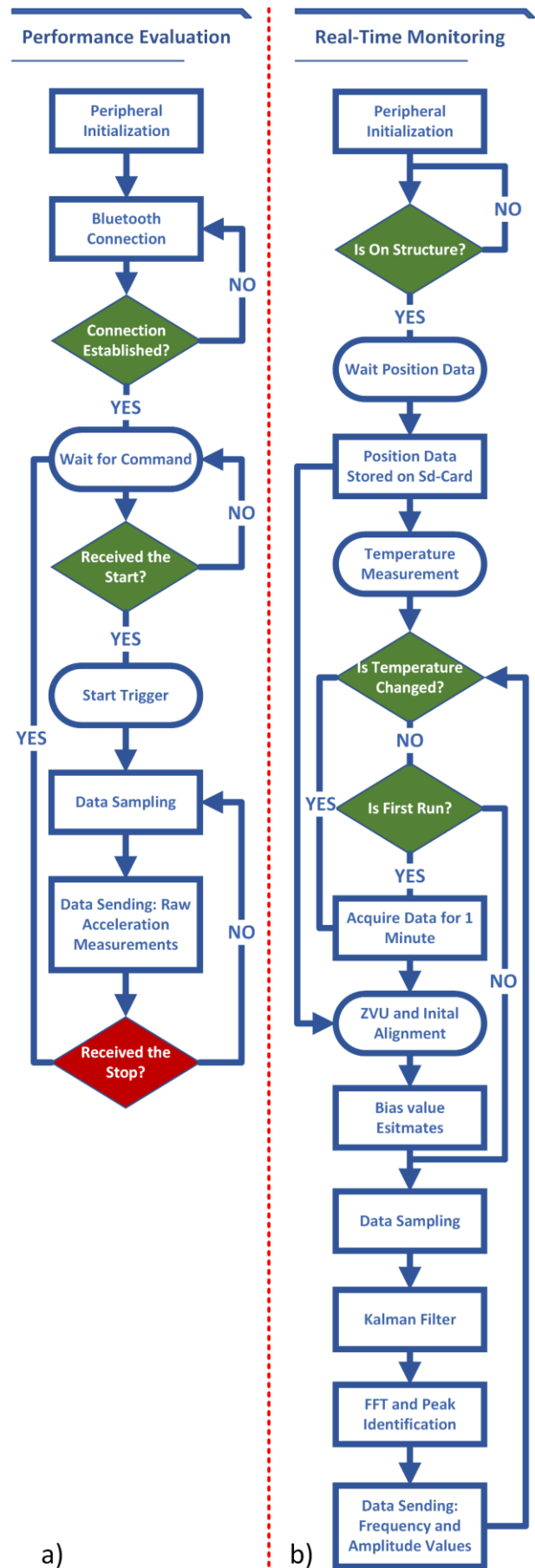


Figure 4. Data acquisition flow-chart for: a) performance evaluation; b) real-time monitoring.

As stated above, the communication between the microcontroller and the PC is realized by means of a Bluetooth protocol (Figure 4.a); this allows control of the start of the acquisition and data collection. Once the start is sent, the microcontroller generates a trigger signal for the sensor modules and starts to acquire data from both. During the tests, it is necessary to ensure accurate measurement synchronizations.

Therefore, the data is processed offline to avoid introducing delays from each data acquisition in both systems. The software architecture is designed with a focus on synchronizing both systems to obtain comparable measurements between the proposed solutions and the reference system. This approach ensures that the results are reliable and can be compared accurately.

As for the wireless sensor node, the software architecture is realized to real-time process the acceleration measurements, as shown in Figure 4b, where the microcontroller acquires data and elaborates them according to the proposed method with the aim to evaluate the maximum frequency peak value and send by means of the LoRaWAN protocol and NFC the oscillation frequency and the associated amplitude values.

The proposed solution is based on the ZVU filter for initial alignment and noise terms evaluation; to enhance parameter estimations require the GNSS position information. To this aim, the realized IoT architecture includes the setting of these parameters that can be stored on the Sd-Card; this procedure could be achieved when the sensor node is mounted on the structure that will not change its position. Finally, the ZVU and initial alignment that requires 60 s is activated in two conditions:

- 1) each time the device is turned on to correct the random bias values;
- 2) whenever the internal temperature of the accelerometer changes by  $\pm 3\text{ }^\circ\text{C}$ , in such a way as to correct the bias values changes due to the temperature.

Once the error values are estimated, the microcontroller removes the high-frequency noise from the raw acceleration measurements adopting the Kalman Filter and then processes them by means of a FFT algorithm to evaluate the maximum frequency peak value and associated amplitude values that are sent through the IoT protocols, i.e., LoRAWAN and NFC.

#### 4. RESULTS

The proposed solution is evaluated according to the measurement setup realized and described in Section 2.1. To this aim, the oscillation measurements in terms of oscillation amplitude of both systems have been compared at different controlled frequencies from 1 Hz to 5 Hz.

The performance of the proposed method has been assessed by comparing the measurement results provided by the realized system with those guaranteed by a marine-grade MEMS sensor, i.e., the STIM318. The raw acceleration measurements are acquired by the concentrator and sent to a PC that collects and processes data by means of a Matlab code, according to Section 2.2.

The performance reached by the proposed method highlights the benefits introduced by exploiting the ZVU filter and initial alignment for measurement calibrations, i.e., the compensation of accelerometer bias drift values. In fact, as shown in Figure 5, the signal spectrum of both systems have been compared, where the amplitude value differences associated with the component at 1 Hz between the proposed method ( $A_{est}$ ) and the reference ( $A_{ref}$ ) are equal to  $0.021\text{ m/s}^2$ , while the amplitude differences

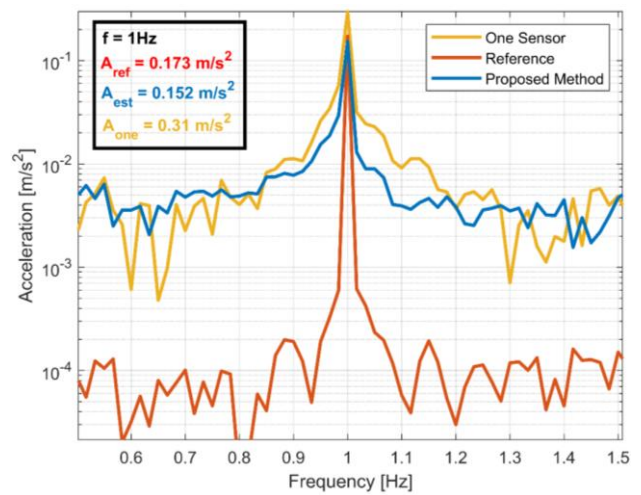


Figure 5. Acceleration amplitude comparison at 1Hz: reference system (red), proposed method (blue) and one sensor measures (orange).

between the best sensor i.e., one cube face ( $A_{one}$ ) measures and reference system are equal to  $0.137\text{ m/s}^2$ . For the sake of clarity, a comparison at frequency oscillation of 1Hz is shown, but similar results have been experienced, which are reported in Table 4. Moreover, the theoretical amplitude values evaluated according to (6) have been reported.

The benefit introduced by the proposed method is highlighted in Table 5, where the differences between the reference system and estimated values ( $\Delta A_{est}$ ) and the reference system and one sensor value ( $\Delta A_{one}$ ) have been reported.

These results are also shown in Figure 6, where the differences between the reference system and uncompensated measures rise as the frequency increases due to the typical low-cost accelerometer errors, while by adopting the proposed method, the differences are constant. In fact, by exploiting the ZVU calibration, the bias drift and bias stability are compensated, as shown by the stability of the system as the frequency increases.

Finally, to assess the proposed solution, Figure 7 shows the second-order polynomial fitting to evaluate the quadratic trend of the acceleration amplitude as the frequency increases. The comparison highlights that the reference system and estimated acceleration amplitude values present a comparable trend with the ideal trend, while instead, the uncompensated values show a significant drift over frequency.

Table 4. Acceleration amplitude results from 1Hz to 5Hz.

Amplitude (m/s <sup>2</sup> )	Oscillation Frequency (Hz)				
	1	2	3	4	5
Reference System	0.173	0.767	1.754	3.123	4.914
Proposed Method	0.152	0.744	1.733	3.101	4.891
One Sensor	0.31	1.243	2.254	4.63	6.823
Theoretical Acceleration	0.197	0.789	1.776	3.158	4.934

Table 5. Amplitude differences between the reference system and (i) the proposed method; (ii) one accelerometer sensor measures.

Amplitude differences (m/s <sup>2</sup> )	Oscillation Frequency (Hz)				
	1	2	3	4	5
$\Delta A_{est}$	0.021	0.023	0.021	0.022	0.022
$\Delta A_{one}$	0.137	0.476	0.5	1.507	1.909

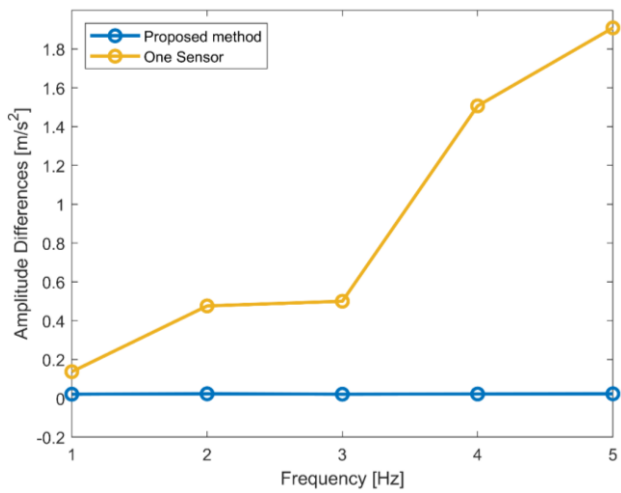


Figure 6. Differences as the frequency changes (from 1 Hz to 5 Hz), between the reference system and (i) the proposed method (blue); (ii) one sensor measures (orange).

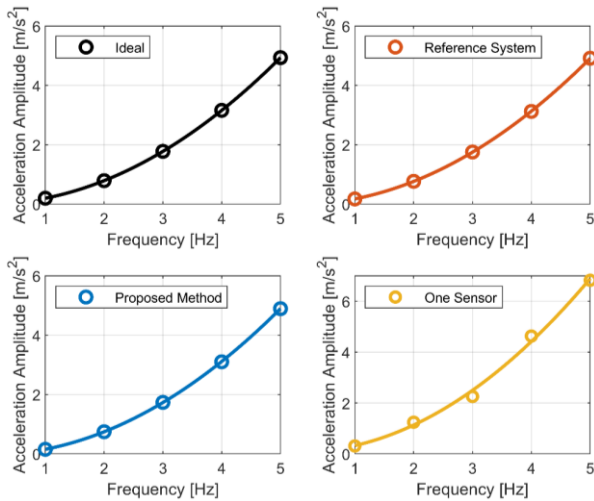


Figure 7. Polynomial fitting comparison: ideal trend (black), reference system (red), proposed method (blue) and, one sensor measure (orange).

Once the performance has been verified, an example of sensor node operation, presented in Section 2.2, is shown in Figure 8. The monitoring dashboard can be accessed from both smartphones and pc, and information regarding the amplitude of the oscillation in g and the frequency is shown. For the sake of clarity, the full dashboard also shows all the sensor axes.

## 5. CONCLUSIONS

The use of MEMS-based sensors in SHM systems has been shown to be an effective and cost-efficient approach for large-scale structural monitoring. However, the inherent errors in MEMS-based sensors can affect the accuracy and reliability of SHM systems. To overcome these challenges, this research evaluates the use of a redundant configuration of low-cost MEMS sensors, then proposes (i) an initialization procedure based on the adoption of a Zero-Velocity Update filter to compensate the bias components i.e., in-run stability, bias instability, and thermal effects; (ii) an initial alignment procedure, and (iii) a Kalman Filter for high-frequency noise reduction that has proven to be effective in improving the performance of MEMS-based SHM systems keeping advantages in terms of

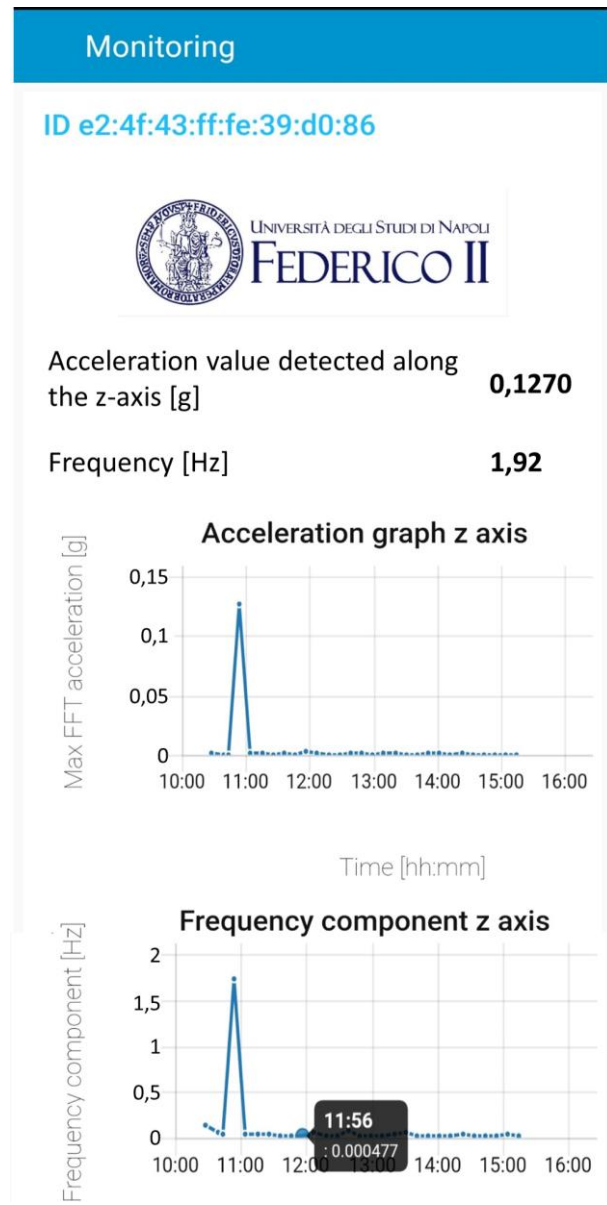


Figure 8. Monitoring dashboard example of operation.

computational load. In particular, the system performance is evaluated by means of a custom oscillating platform that provides oscillation at constant displacement and variable frequency. In this way, the proposed method is tested, and a comparison with a reference system, i.e., a marine-grade accelerometer, theoretical values, and the one accelerometer sensor measures, has been evaluated. The proposed method highlights a remarkable agreement with the reference system, which respects the theoretical trend, and the performance improvements over one accelerometer sensor measurements are deduced from the results obtained; in fact, amplitude differences of  $0.02 \text{ m/s}^2$  and  $0.137 \text{ m/s}^2$  have been experienced between the reference system and the proposed solution and one sensor respectively. Moreover, it is observed that drift and bias stability errors are not present in the system as the frequency increases.

Finally, a smart monitoring architecture has been proposed based on the adoption of a sensor node capable of real-time monitoring of the structure by exploiting the IoT communication protocols, i.e., LoRAWAN and NFC. The use of these systems, combined with the proposed solution, can

provide accurate and reliable data, leading to timely maintenance and cost savings.

As future work, additional tests will be executed by means of different beam sizes (the acceleration amplitude could be changed by modifying the beam length) and a vibrodyne to suitably assess the combined effects of amplitude and frequency by evaluating the minimum and maximum operating values.

## REFERENCES

- [1] L. Sun, Z. Shang, Y. Xia, S. Bhowmick, S. Nagarajaiah, Review of bridge structural health monitoring aided by big data and artificial intelligence: From condition assessment to damage detection, *Journal of Structural Engineering*, vol. 146, no. 5, 2020, p. 4020073.  
DOI: [10.1061/\(ASCE\)ST.1943-541X.0002535](https://doi.org/10.1061/(ASCE)ST.1943-541X.0002535)
- [2] J. Seo, J. W. Hu, J. Lee, Summary review of structural health monitoring applications for highway bridges, *Journal of Performance of Constructed Facilities*, vol. 30, no. 4, 2016, p. 4015072.  
DOI: [10.1061/\(ASCE\)CF.1943-5509.0000824](https://doi.org/10.1061/(ASCE)CF.1943-5509.0000824)
- [3] F. Lamonaca, C. Scuro, D. Grimaldi, R. S. Olivito, P. F. Sciammarella, D. L. Carni, A layered IoT-based architecture for a distributed structural health monitoring system System, *Acta IMEKO*, vol. 8, no. 2, 2019, pp. 45–52.  
DOI: [10.21014/acta\\_imeko.v8i2.640](https://doi.org/10.21014/acta_imeko.v8i2.640)
- [4] N. Giulietti, P. Chiariotti, G. Cosoli, G. Giacometti, L. Violini, A. Mobili, G. Pandarese, F. Tittarelli, G. M. Revel, Continuous monitoring of the health status of cement-based structures: electrical impedance measurements and remote monitoring solutions, *Acta IMEKO*, vol. 10, no. 4, 2021, pp. 132–139.  
DOI: [10.21014/acta\\_imeko.v10i4.1140](https://doi.org/10.21014/acta_imeko.v10i4.1140)
- [5] A. Cigada, L. Corradi Dell'Acqua, B. Mörlin Visconti Castiglione, M. Scaccabarozzi, M. Vanali, E. Zappa, Structural health monitoring of an historical building: the main spire of the Duomo Di Milano. *International Journal of Architectural Heritage*, vol. 11, no. 4, pp. 501–518, 2017.  
DOI: [10.1080/15583058.2016.1263691](https://doi.org/10.1080/15583058.2016.1263691)
- [6] M. Carratù, V. Gallo, V. Paciello, A. Pietrosanto, A deep learning approach for the development of an Early Earthquake Warning system, *IEEE Int. Instrumentation and Measurement Technology Conf. (I2MTC)*, Ottawa, ON, Canada, 16-19 May 2022, pp. 1–6.  
DOI: [10.1109/I2MTC48687.2022.9806627](https://doi.org/10.1109/I2MTC48687.2022.9806627)
- [7] L. Angrisani, F. Bonavolontà, G. d'Alessandro, M. D'Arco, Inductive power transmission for wireless sensor networks supply, *IEEE Workshop on Environmental, Energy, and Structural Monitoring Systems*, Naples, Italy, 17-18 September 2014, pp. 1-5.  
DOI: [10.1109/EESMS.2014.6923289](https://doi.org/10.1109/EESMS.2014.6923289)
- [8] C. Scuro, P. F. Sciammarella, F. Lamonaca, R. S. Olivito, D. L. Carni, IoT for structural health monitoring, *IEEE Instrum Meas Mag*, vol. 21, no. 6, 2018, pp. 4–14.  
DOI: [10.1109/MIM.2018.8573586](https://doi.org/10.1109/MIM.2018.8573586)
- [9] A. Astarita, F. Tucci, A. T. Silvestri, M. Perrella, L. Boccarusso, P. Carlone, Dissimilar friction stir lap welding of AA2198 and AA7075 sheets: forces, microstructure and mechanical properties, *Int. Journal of Advanced Manufacturing Technology*, 117, 2021, pp 1045–1059.  
DOI: [10.1007/s00170-021-07816-7](https://doi.org/10.1007/s00170-021-07816-7)
- [10] F. Tucci, P. Carlone, A. T. Silvestri, H. Parmar, A. Astarita, Dissimilar friction stir lap welding of AA2198-AA6082: Process analysis and joint characterization, *CIRP J Manuf Sci Technol*, vol. 35, 2021, pp. 753–764.  
DOI: [10.1016/j.cirpj.2021.09.007](https://doi.org/10.1016/j.cirpj.2021.09.007)
- [11] P. Jiao, K.-J. I. Egbe, Y. Xie, A. Matin Nazar, A. H. Alavi, Piezoelectric sensing techniques in structural health monitoring: A state-of-the-art review, *Sensors*, vol. 20, no. 13, 2020, p. 3730.  
DOI: [10.3390/s20133730](https://doi.org/10.3390/s20133730)
- [12] I. Roselli, A. Tatì, V. Fioriti, I. Bellagamba, M. Mongelli, R. Romano, G. De Canio, M. Barbera, M. Cianetti, Integrated approach to structural diagnosis by non-destructive techniques: The case of the Temple of Minerva Medica, *Acta IMEKO*, vol. 7, no. 3, 2018, pp. 13–19.  
DOI: [10.21014/acta\\_imeko.v7i3.558](https://doi.org/10.21014/acta_imeko.v7i3.558)
- [13] F. Zonzini, C. Aguzzi, L. Gigli, L. Sciuillo, N. Testoni, L. De Marchi, M. Di Felice, T. S. Cinotti, C. Mennuti, A. Marzani, Structural Health Monitoring and Prognostic of Industrial Plants and Civil Structures: A Sensor to Cloud Architecture, *IEEE Instrum Meas Mag*, vol. 23, no. 9, 2020, pp. 21–27.  
DOI: [10.1109/MIM.2020.9289069](https://doi.org/10.1109/MIM.2020.9289069)
- [14] D. Seneviratne, L. Ciani, M. Catelani, D. Galar, Smart maintenance and inspection of linear assets: An Industry 4.0 approach, *Acta IMEKO*, vol. 7, no. 1, 2018, pp. 50-56.  
DOI: [10.21014/acta\\_imeko.v7i1.519](https://doi.org/10.21014/acta_imeko.v7i1.519)
- [15] C. R. Farrar, K. Worden, An introduction to structural health monitoring, *Philosophical Transactions of the Royal Society A: Mathematical, Physical and Engineering Sciences*, vol. 365, no. 1851, 2007, pp. 303–315.  
DOI: [10.1098/rsta.2006.1928](https://doi.org/10.1098/rsta.2006.1928)
- [16] P. Rizzo, A. Enshaian, Challenges in bridge health monitoring: A review, *Sensors*, vol. 21, no. 13, 2021, p. 4336.  
DOI: [10.3390/s21134336](https://doi.org/10.3390/s21134336)
- [17] P. J. Vardanega, G. T. Webb, P. R. A. Fidler, F. Huseynov, K. Kariyawasam, C. R. Middleton, Bridge monitoring, In: *Innovative bridge design handbook*, Elsevier, 2022, pp. 893–932.  
DOI: [10.1016/B978-0-12-823550-8.00023-8](https://doi.org/10.1016/B978-0-12-823550-8.00023-8)
- [18] L. Ciani, A. Bartolini, G. Guidi, G. Patrizi, A hybrid tree sensor network for a condition monitoring system to optimise maintenance policy, *Acta IMEKO*, vol. 9, no. 1, 2020, pp. 3–9.  
DOI: [10.21014/acta\\_imeko.v9i1.732](https://doi.org/10.21014/acta_imeko.v9i1.732)
- [19] M. Brambilla, P. Chiariotti, F. Di Carlo, P. Isabella, A. Meda, P. Darò, A. Cigada, Metrological Evaluation of New Industrial SHM Systems Based on MEMS and Microcontrollers, *European Workshop on Structural Health Monitoring: EWSHM 2022, Volume 1*, Springer, 2022, pp. 774–783.  
DOI: [10.1007/978-3-031-07254-3\\_78](https://doi.org/10.1007/978-3-031-07254-3_78)
- [20] A. Liccardo, F. Bonavolontà, M. Balato, C. Petrarca, Lora-Based Smart Sensor for PD Detection in Underground Electrical Substations, *IEEE Trans Instrum Meas*, vol. 71, 2022, pp. 1–13.  
DOI: [10.1109/TIM.2022.3200427](https://doi.org/10.1109/TIM.2022.3200427)
- [21] E. Reynders, System identification methods for (operational) modal analysis: review and comparison, *Archives of Computational Methods in Engineering*, vol. 19, no. 1, 2012, pp. 51–124.  
DOI: [10.1007/s11831-012-9069-x](https://doi.org/10.1007/s11831-012-9069-x)
- [22] A. Lavatelli, E. Zappa, Uncertainty in vision based modal analysis: probabilistic studies and experimental validation, *Acta IMEKO*, vol. 5, no. 4, 2016, pp. 37–48.  
DOI: [10.21014/acta\\_imeko.v5i4.426](https://doi.org/10.21014/acta_imeko.v5i4.426)
- [23] G. Cerro, L. Ferrigno, M. Laracca, F. Milano, P. Carbone, A. Comuniello, A. De Angelis, A. Moschitta, An accurate localization system for nondestructive testing based on magnetic measurements in quasi-planar domain, *Measurement*, vol. 139, 2019, pp. 467–474.  
DOI: [10.1016/j.measurement.2019.03.022](https://doi.org/10.1016/j.measurement.2019.03.022)
- [24] R. R. Ribeiro, R. de M. Lameiras, Evaluation of low-cost MEMS accelerometers for SHM: frequency and damping identification of civil structures, *Latin American Journal of Solids and Structures*, vol. 16, 2019.  
DOI: [10.1590/1679-78255308](https://doi.org/10.1590/1679-78255308)
- [25] F. Bonavolontà, L. P. Di Noia, A. Liccardo, S. Tessitore, D. Lauria, A PSO-MMA Method for the Parameters Estimation of Interarea Oscillations in Electrical Grids, *IEEE Trans Instrum Meas*, vol. 69, no. 11, 2020.  
DOI: [10.1109/TIM.2020.2998909](https://doi.org/10.1109/TIM.2020.2998909)
- [26] R. Iervolino, F. Bonavolontà, A. Cavallari, A wearable device for sport performance analysis and monitoring, in *2017 IEEE International Workshop on Measurement and Networking, M and N 2017*, Naples, Italy, 27-29 September 2017, pp. 1-6.  
DOI: [10.1109/IWMN.2017.8078375](https://doi.org/10.1109/IWMN.2017.8078375)
- [27] M. Varanis, A. Silva, A. Mereles, R. Pederiva, MEMS accelerometers for mechanical vibrations analysis: A compre-

- hensive review with applications, *Journal of the Brazilian Society of Mechanical Sciences and Engineering*, vol. 40, 2018, pp. 1–18. DOI: [10.1007/s40430-018-1445-5](https://doi.org/10.1007/s40430-018-1445-5)
- [28] C. Bedon, E. Bergamo, M. Izzi, S. Noè, Prototyping and validation of MEMS accelerometers for structural health monitoring - The case study of the Pietratagliata cable-stayed bridge, *Journal of Sensor and Actuator Networks*, vol. 7, no. 3, 2018, p. 30. DOI: [10.3390/jsan7030030](https://doi.org/10.3390/jsan7030030)
- [29] S. Han, Z. Meng, O. Omisore, T. Akinyemi, Y. Yan, Random error reduction algorithms for MEMS inertial sensor accuracy improvement - a review, *Micromachines*, vol. 11, no. 11, 2020, 36 pp. DOI: [10.3390/mi11111021](https://doi.org/10.3390/mi11111021)
- [30] H. Huang, H. Zhang, L. Jiang, An Optimal Fusion Method of Multiple Inertial Measurement Units Based on Measurement Noise Variance Estimation, *IEEE Sens J*, vol. 23, no. 3, 2023, pp. 2693–2706. DOI: [10.1109/JSEN.2022.3229475](https://doi.org/10.1109/JSEN.2022.3229475)
- [31] S. Ahvenjärvi, The Human Element and Autonomous Ships, *TransNav, the International Journal on Marine Navigation and Safety of Sea Transportation*, vol. 10, no. 3, 2017, pp. 517-521. DOI: [10.12716/1001.10.03.18](https://doi.org/10.12716/1001.10.03.18)
- [32] P. D. Groves, Principles of GNSS, inertial, and multisensor integrated navigation systems, 2nd edition [Book review], *IEEE Aerospace and Electronic Systems Magazine*, vol. 30, no. 2, 2015, pp. 26 - 27. DOI: [10.1109/MAES.2014.14110](https://doi.org/10.1109/MAES.2014.14110)
- [33] G. T. Schmidt, INS/GPS Technology Trends, *Technology (Singap World Sci)*, vol. 116, no. 2010, 2011.
- [34] G. de Alteriis, V. Bottino, C. Conte, G. Rufino, R. S. Lo Moriello, Accurate Attitude Initialization Procedure based on MEMS IMU and Magnetometer Integration, 2021 IEEE 8th Int. Workshop on Metrology for AeroSpace (MetroAeroSpace), Naples, Italy, 23-25 June 2021, pp. 1–6. DOI: [10.1109/MetroAeroSpace51421.2021.9511679](https://doi.org/10.1109/MetroAeroSpace51421.2021.9511679)
- [35] A. Liccardo, S. Tessitore, F. Bonavolontà, S. Cristiano, L. P. D. Noia, G. M. Giannuzzi, C. Pisani, Detection and Analysis of Inter-Area Oscillations Through a Dynamic-Order DMD Approach, *IEEE Trans Instrum Meas*, vol. 71, 2022, pp. 1–14. DOI: [10.1109/TIM.2022.3186371](https://doi.org/10.1109/TIM.2022.3186371)
- [36] R. Alfian, A. Ma'arif, S. Sunardi, Noise Reduction in the Accelerometer and Gyroscope Sensor with the Kalman Filter Algorithm, *Journal of Robotics and Control (JRC)*, vol. 2, Nov. 2020, pp. 180–189. DOI: [10.18196/jrc.2375](https://doi.org/10.18196/jrc.2375)
- [37] D. Capriglione, M. Carratù, M. Catelani, L. Ciani, G. Patrizi, A. Pietrosanto, P. Sommella, Experimental Analysis of Filtering Algorithms for IMU-Based Applications under Vibrations, *IEEE Trans Instrum Meas*, vol. 70, 2021, pp. 1-10. DOI: [10.1109/TIM.2020.3044339](https://doi.org/10.1109/TIM.2020.3044339)
- [38] F. Bonavolontà, M. D'Arco, A. Liccardo, O. Tamburisi, Remote laboratory design and implementation as a measurement and automation experiential learning opportunity, *IEEE Instrum Meas Mag*, vol. 22, no. 6, 2019, pp. 62–67. DOI: [10.1109/MIM.2019.8917906](https://doi.org/10.1109/MIM.2019.8917906)
- [39] D. Capriglione, G. Cerro, L. Ferrigno, G. Miele, Analysis and implementation of a wavelet based spectrum sensing method for low SNR scenarios, 2016 IEEE 17th Int. Symposium on a World of Wireless, Mobile and Multimedia Networks (WoWMoM), IEEE, Coimbra, Portugal, 21-24 June 2016, pp. 1–6. DOI: [10.1109/WoWMoM.2016.7523585](https://doi.org/10.1109/WoWMoM.2016.7523585)
- [40] G. de Alteriis, A. T. Silvestri, V. Bottino, E. Caputo, F. Bonavolontà, R. S. Lo Moriello, A. Squillace, D. Accardo, Innovative Fusion Strategy for MEMS Redundant-IMU Exploiting Custom 3D Components, 2022 IEEE 9th Int. Workshop on Metrology for AeroSpace (MetroAeroSpace), Pisa, Italy, 27-29 June 2022, pp. 644–648. DOI: [10.1109/MetroAeroSpace54187.2022.9856222](https://doi.org/10.1109/MetroAeroSpace54187.2022.9856222)
- [41] A. T. Silvestri, I. Papa, F. Rubino, A. Squillace, On the Critical Technological Issues of CFF: Enhancing the Bearing Strength, *Materials and Manufacturing Processes*, vol. 37, no. 2, 2022, pp. 123-135. DOI: [10.1080/10426914.2021.1954195](https://doi.org/10.1080/10426914.2021.1954195)
- [42] A. T. Silvestri, I. Papa, A. Squillace, Influence of Fibre Fill Pattern and Stacking Sequence on Open-Hole Tensile Behaviour in Additive Manufactured Fibre-Reinforced Composites, *Materials*, vol. 16, no. 6, 2023, 13 pp. DOI: [10.3390/ma16062411](https://doi.org/10.3390/ma16062411)